ELSEVIER

Effects of electrospinning parameters on polyacrylonitrile nanofiber diameter: An investigation by response surface methodology

O.S. Yördem [1], M. Papila *, Y.Z. Menceloğlu [2]

Faculty of Engineering and Natural Sciences, Sabancı University, Orhanlı Tuzla, 34956 Istanbul, Turkey

Abstract

Effects of material and process parameters on the diameter of electrospun polyacrylonitrile fibers were experimentally investigated. Response surface methodology (RSM) was utilized to design the experiments at the settings of solution concentration, voltage and the collector distance. It also imparted the evaluation of the significance of each parameter on the resultant fiber diameter. The investigations were carried out in the two-variable process domains of several collector distances as applied voltage and the solution concentration were varied at a fixed polymer molecular weight. The mean diameter and coefficient of variation were modeled by polynomial response surfaces as functions of solution concentration and voltage at each collector distance. Effect of applied voltage in micron-scale fiber diameter was observed to be almost negligible when solution concentration and collector distance were high. However, all three factors were found statistically significant in the production of nano-scale fibers. The response surface predictions revealed the parameter interactions for the resultant fiber diameter, and showed that there is a negative correlation between the mean diameter and coefficient of variation for the fiber diameter. A sub-domain of the parameter space consisting of the solution concentration, applied voltage and collector distance, was suggested for the potential nano-scale fiber production.
© 2007 Elsevier Ltd. All rights reserved.

Keywords: Nanofiber; Electrospinning; Response surface methodology

1. Introduction

Nanomaterials have become a research priority as biotechnology, defense and semiconductor industries in particular, are interested in potential applications of nanotechnology. Specifically, a substantial amount of research on nano-scale fibers is being conducted to meet the demands of their prospective application areas such as tissue engineering [1,2], membranes [3], nano-resonators [4], micro-air vehicles [5], and hydrophobic thin films [6].

Electrospinning (also called electrostatic fiber spinning) has been one of the promising processes to produce continuous nano-scale fibers from both synthetic and natural polymers. Electric forces are used to form fibers from material solutions or melts in the electrospinning process. Studies on electrically driven liquid jets were initially started in 19th century, and electrospinning of polymer fibers was first patented by Formhals in 1934 [7]. The main principle in electrospinning as defined by Doshi and Reneker is to generate a charged jet of polymeric solution by applying an electric field [8,9]. As the jet travels in the air, the solvent evaporates and a charged fiber is left behind which can be collected on a grounded plate (collector). Through this process, mostly mats of randomly oriented fibers with large surface to volume ratio as well as various fiber morphologies and geometries are fabricated from various polymer solutions, as noted in Deitzel et al. [10]. Theoretical simulation of the process, fiber formation mechanism, parameters

---

* Corresponding author. Tel.: +90 216 483 9546; fax: +90 216 483 9550.
 E-mail addresses: sinanyordem@su.sabanciuniv.edu (O.S. Yördem), mpapila@sabanciuniv.edu (M. Papila), yusufm@sabanciuniv.edu (Y.Z. Menceloğlu).
 [1] Tel.: +90 216 483 9000/2079; fax: +90 216 483 9550.
 [2] Tel.: +90 216 483 9535; fax: +90 216 483 9550.

influencing the fiber dimension and morphology have been under extensive investigation for the last decade [8,10–18]. Up-to-date achievements in fiber production via electrospinning were well summarized by Dzenis [19]. He highlighted, for instance, highly aligned fibers and their assemblies made possible by understanding and controlling the bending instabilities. He also addressed new challenges such as analysis of the effects of solvent evaporation that may help to develop robust methods for manufacturing extremely small nanofibers.

The resultant fiber diameter determines properties of the electrospun fiber mats such as mechanical, electrical, and optical properties. It was previously shown that both the strength and the conductivity of the film/mat of fibers produced by electrospinning are sensitive to fiber diameter [20,21]. Moreover, size of the fibers along with morphology influences the hydrophobic behavior of polymers. Acatay et al. [6] illustrated the effect of morphology of the electrospun mat of crosslinked polyacrylonitrile (PAN) fibers on the resultant hydrophobic behavior. They observed three different morphologies: beads only, beads-on-fibers and fibers only. Following their work, Simsek et al. [22] concluded that water contact angles (hydrophobic surface) are affected by the size of fibers. Filtering application is also affected by the fiber size [23,24]. Therefore, it is important to have control over the fiber diameter which is a function of material and process parameters. Despite relatively early introduction of the electrospinning process, the effects of the process and material parameters on the fiber formation are still under investigation theoretically and experimentally. Fridrikh et al. [14] derived an expression for the diameter of the jet, generated as a function of material properties such as conductivity, dielectric permittivity, dynamic viscosity, surface tension, and density; as well as process characteristics (e.g. flow rate, applied electric field, and electric current). Their predictions correlated very well with the experimental results for polyethyleneoxide (PEO) and moderately with the results for PAN. Sukigara et al. [17] have reported an experimental work via response surface methodology (RSM), and shown that the effect of the applied voltage creating the electric field may be surprisingly small or expectedly significant depending on the solution concentration in electrospinning of Bombyx Mori silk. Their work sets a good example of the possible interactions between the parameters of the process that may also be expected for other polymers. Gu et al. [25] who also employed RSM, reported no significant effect of voltage on the processing of commercially available PAN for nanofibers. Their experiments, however, were at a constant collector distance whose possible interaction with the other parameters may not have surfaced in their results.

The objective of this study was to investigate the electrospinning related material and process parameters, solution concentration, applied voltage and collector distance, and their individual and interactive effects on the PAN

fiber diameter. Another aim was to predict the domain of the parameters where targeted PAN fiber diameter can be achieved. In this experiment-oriented work, PAN polymer solution was electrospun to produce nano-scale fibers, and emphasis was given to the effect of polymer solution concentration, applied voltage, and the collector distance. Their effects were investigated within the context of response surface methodology (RSM) that incorporates design of experiments (DOE) and linear regression [26–28]. This approach enables experimental investigation of the individual factors and the interactions of the factors (variables or parameters) simultaneously [13,17,25] as opposed to one factor at-a-time approach [10,29–31]. A surrogate model of fiber diameter that is a response surface approximation was constructed. Such an empirical model allows the evaluation of significance of the parameters based on experimental results for the fiber diameter and provides prediction capability for the process domain of targeted fiber diameter.

2. Experimental procedure

2.1. Description of "experiment" for the present work

In this experiment-oriented study an "experiment" has the following set of actions: (i) polymer preparation, (ii) electrospinning of the polymer, and (iii) scanning electron microscopy (SEM) imaging of the collected mat of fibers and image processing to determine fiber diameter statistics. The experiment parameters or variables were considered as material related variables (e.g., molecular weight and solution concentration) and process related variables (e.g., applied voltage and collector distance) and the result of the experiment is the electrospun fiber diameter.

2.1.1. Nano-scale fiber material: preparation of PAN–DMF polymer solution

Polyacrylonitrile was the polymer of interest in this work. It was synthesized by solution polymerization at Sabancı University Polymer Synthesis Laboratory. The acrylonitrile (AN, Merck) was used after purification by double distillation over CaH_2 under nitrogen. N,N-Dimethylformamide (DMF, Labscan) and azo-bis-isobutyronitrile (AIBN, Fluka) were used as received. Molecular weight of PAN was adjusted by changing AIBN concentration and fixing the amount of AN concentration. The syntheses of the two polymers having different molecular weights labeled as high (HMW) and low (LMW) are summarized in Table 1. Reported viscosity average molecular weights were measured with Ubbelohde Viscometer, by preparing solutions in DMF at 25 °C and calculated by the Mark-Houwink equation with K' and a constants 0.052 and 0.690, respectively [32].

After fixing the molecular weight of the PAN as described in Table 1, the polymer was dissolved in DMF and stirred for 24 h. As a result, homogenous HMW PAN–DMF and LMW PAN–DMF solutions in different concentrations ranging between 8% and 16% (w/w- weight-by-weight basis) were prepared.

Table 1
Synthesis of PAN, and viscosity average molecular weight of each sample

Sample	Amount of			MW_v (g/mol)
	AN (g)	AIBN (g)	DMF (ml)	
HMW	10	0.0019	20	121,000
LMW	10	0.0087	20	73,400

2.1.2. Nano-scale fiber production by electrospinning: process description

Polymer fibers of nano and sub-micron scale were manufactured by electrospinning process, the setup for which is schematically represented in Fig. 1. The polymer solution was placed into a syringe/capillary tube connected to a high voltage source. An electric field is formed between the grounded collector and the tip of the syringe/capillary tube (1.13 mm in diameter). A syringe pump (Univentor 801 Syringe Pump) was utilized to form a constant amount of solution on the tip. The resultant electrostatic forces cause the ejection of the polymer solution to air forming a jet. As the polymer solution jet travels in the air, the solvent evaporates, and the polymer is collected on the grounded conductive target as fine fibers [8]. This stationary collection procedure results in non-woven fiber mats as seen in Fig. 1.

2.1.3. Measurements: dimensional characterization of non-woven fiber mats

Primary focus was on the effects of material and process parameters on the fiber diameter and its statistics over each non-woven fiber mat. After formation the non-woven mat of fibers on the aluminum collector, several images from each mat sample were taken by SEM (LEO 1530VP). Images taken relatively apart from each other were considered, and diameter measurements of about a total of 50 fibers, each with multiple sampling, were carried out. An image processing software (MediaCybernetics, Image Pro Plus 5.1) was used to make the measurements. This sampling scheme was to catch the scattering of the fiber dimensional characteristics over the whole non-woven fiber mat. It enabled the determination of statistics for fiber diameter (mean, standard deviation and distribution) on each SEM sample image. A typical distribution of measured fiber diameters is shown in Fig. 2.

2.2. Planning and analysis of experiments: response surface methodology

Investigation of the electrospinning process and its effects on the PAN fiber diameter requires a number of experiments described in the previous section. The planning and analysis of these experiments were performed within the context of Response Surface methodology. Response surfaces (RS) are in fact used to approximate numerical or physical experimental data by an expression that is usually a low-order polynomial. The three key steps of the methodology as noted in [27] are the following:
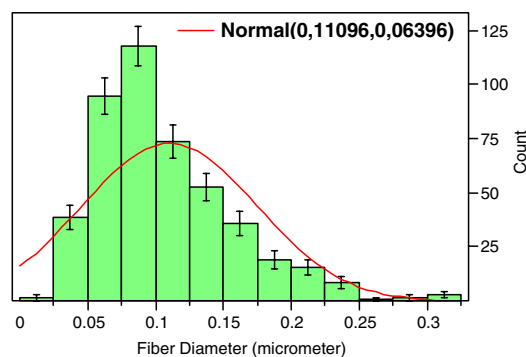

Fig. 2. Fiber diameter distribution for HMW, 8% solution concentration, 20 kV voltage and 8 cm collector distance.

2.2.1. Design of experiments

Parameter or factor settings at which the experiments were conducted were pre-selected. The selection represents the design/parameter space so that the experiments will yield adequate and reliable measurements/calculations of the response of interest. Two-level and three-level factorial experimental designs were used in this study for four and two variable/parameter cases, respectively, as described in the following sections.

2.2.2. Regression analysis

A mathematical approximation model was determined, which was fit to the data that was generated from the set of experiment points of the previous step. The fundamentals for the least squares fitting procedure can be found in number of sources [27], but are also briefly introduced here as an appendix. The regression analysis was performed using a statistical software JMP IN 5.1 by SAS Institute. The software also conducts appropriate statistical test of hypotheses (see Appendix) concerning the parameters in the mathematical model that is the RS approximation.

2.2.3. Prediction of experiment settings for specified response

The response was predicted at a given set of the experimental factors/variables by using the RS approximation. The specific settings or domain of the factors/parameters that produce extremums (maximum or
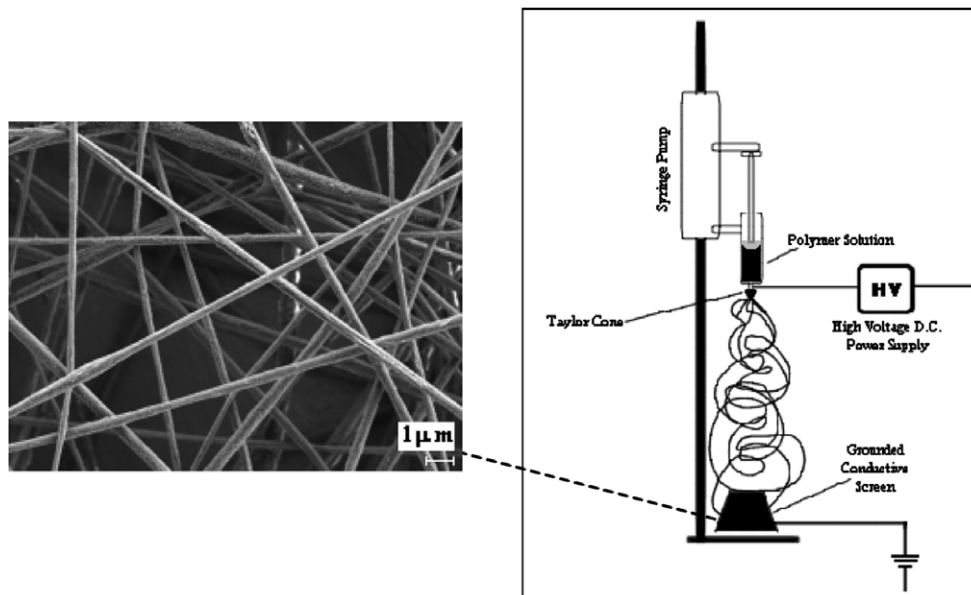

Fig. 1. Electrospinning setup and its product: non-woven fiber mat.

minimum) or targeted value of the response can be determined. This can be easily achieved by graphical means in one-variable and two-variable cases. For higher dimensional problems, numerical optimization techniques are usually applied.

3. Screening for significant parameters in electrospinning of polymer fibers

A preliminary screening study was first carried out in order to rank the significance of four major parameters on the resultant mean diameter of the polymer fibers collected by electrospinning. The total of four parameters consists of two material and two process related factors: molecular weight and solution concentration of the polymer, and applied DC voltage and the collector distance, respectively. The selected experimental design was two-level factorial experimental design and provided 16 experiment settings for four variables. The experiment settings were the vertices of a four-dimensional cuboidal region formed by the combinations of lower and upper limits of each parameter, as summarized in Table 2.

Experimental procedure described in the previous section was applied at each of the 16 settings $(x_1^L, x_2^L, x_3^L, x_4^L)$, $(x_1^L, x_2^L, x_3^L, x_4^U)$, $(x_1^L, x_2^L, x_3^U, x_4^L), \ldots, (x_1^U, x_2^U, x_3^U, x_4^U)$. Following the fiber production, statistics of the fiber diameter sampled on SEM images from each non-woven mat were computed. Among the mats of the 16 settings sampled, the minimum fiber diameter was observed at the parameter settings of $(x_1^L, x_2^U, x_3^U, x_4^L)$ as 0.434 ± 0.188 μm and the maximum was at $(x_1^U, x_2^L, x_3^L, x_4^U)$ as 2.946 ± 1320 μm.

Next, regression analysis was performed to fit the observed response y, the mean fiber diameter. The true, but unknown relation between the mean fiber diameter and the parameters $\eta = f(x_1, x_2, x_3, x_4)$ was approximated by a first-order polynomial model in four variables and denoted as $\hat{y}$,

$$\hat{y} = b_0 + b_1 x_1 + b_2 x_2 + b_3 x_3 + b_4 x_4 \tag{1}$$

The unknown coefficients in Eq. (1) were found by JMP IN, which employs the least squares method described in Appendix. Table 3 presents the summary of the statistics from the data and first-order polynomial model. The second column reports the estimates of the coefficients in Eq. (1) (see Eq. (6) in Appendix). Measure of goodness of the fit, R^2 via Eq. (8) (unity suggests perfect fit), is about 0.9, which is a statistical indication that the variation in the fiber diameter is explained reasonably well by the model in Eq. (1).

Table 2
Material and process parameters for significance screening and upper and lower limits used in the two-level factorial experimental design

Variable	Variable description	Lower limit x_i^L	Upper limit x_i^U
x_1	Molecular weight[a] (g/mol)	73,400	121,000
x_2	Solution concentration (%)	12	16
x_3	Applied voltage (kV)	12	16
x_4	Collector distance (cm)	12	16

[a] Computed HMW and LMW values for the polymer synthesis summarized in Table 1.

Table 3
Statistics of first order polynomial approximation Eq. (1), fit to mean fiber diameter data after screening tests for four parameters

Term	Estimate	Prob > t	Summary of fit	
Intercept, $b0$	-2.84×10^0	0.016	Mean, $\bar{y}$	1.388
Molecular weight, $b1$	3.13×10^{-5}	<0.001	RMSE	0.311
Concentration, $b2$	-3.04×10^{-2}	0.451	R^2	0.899
Voltage, $b3$	9.20×10^{-2}	0.038		
Distance, $b4$	2.34×10^{-2}	0.560		

The other reported statistics, p-values associated with the coefficient estimates are statistical measures of significance of the individual parameters in explaining the variability of the fiber diameter over the cuboidal domain. The lower the p-value, the more significant the parameter is.

The p-values of the parameter estimates are below the significance level of 0.05;[3] therefore, Table 3 suggests that molecular weight x_1 and applied voltage x_3 are significant factors for the variation of the fiber diameter. For the other two factors, solution concentration and the collector distance, there is no strong statistical evidence that the coefficients are different than zero as the p-values are substantially high.

The significance of the molecular weight and voltage is not surprising [13,15,29]. Other variables, however, were also expected to play a role in fiber formation as demonstrated by Demir et al. [18] for polyurethane fibers, and by Sukigara et al. [17] for Bombyx silk fibers of fixed molecular weight. The varied molecular weight, however, seems to be a dominant factor and explains most of the variation around the mean of the 16 measured mean-fiber diameters, $\bar{y}$ in the studied ranges of Table 2. Dominancy of the molecular weight was expected because it is the molecular weight which affects the entanglement of the polymer chains and it is the stretching of the polymer solution that preserves a continuous solution jet to form fibers [33].

Note that the first-order model was not intended to predict the fiber diameter within the four dimensional cuboidal domain. This is firstly because of the fact that the given domain where the model is valid does not seem to provide nano-scale fiber diameter contrary to the objective of this study. And secondly, higher order model is usually necessary to make more precise predictions; therefore, additional experiments at other levels of parameters are also required.

4. Prediction of domain of experimental settings for nano-scale fibers

The screening experiments demonstrated that fiber diameter in the selected range of the parameters is mostly

---

[3] p-Value below 0.05 means that the probability of being wrong in accepting that b_1 and b_3 coefficients are different than zero will be less than 5%. This shows x_1 and x_3 as the significant factors.

Table 4
Experiments at each collector distance, in the extended two-variable, solution concentration and applied voltage domain (the molecular weight is fixed, $x_1 = 73,413$)

Experiment	Collector Distance, x_4: 8, 12, 16 cm		Mean Diamater $\pm$ std. dev (μm)		
	Solution concent., x_2 (%)	Applied voltage, x_3 (kV)	at $x_4 = 8$ cm	at $x_4 = 12$ cm	at $x_4 = 16$ cm
1	8	10	0.083 ± 0.039	0.166 ± 0.058	0.137 ± 0.065
2	8	20	0.109 ± 0.065	0.093 ± 0.040	0.162 ± 0.111
3	8	30	1.592 ± 0.473	0.084 ± 0.033	0.124 ± 0.041
4	10	15	0.773 ± 0.403	0.244 ± 0.086	0.171 ± 0.101
5	10	25	0.955 ± 0.440	0.326 ± 0.107	0.339 ± 0.127
6	12	10	0.920 ± 0.360	0.625 ± 0.305	0.714 ± 0.205
7	12	20	0.556 ± 0.226	0.548 ± 0.209	0.540 ± 0.173
8	12	30	0.548 ± 0.243	0.635 ± 0.383	0.561 ± 0.166
9	14	15	0.804 ± 0.350	1.608 ± 0.731	0.880 ± 0.222
10	14	25	0.942 ± 0.409	1.569 ± 0.474	1.127 ± 0.378
11	16	10	1.933 ± 0.655	1.756 ± 0.586	2.694 ± 0.696
12	16	20	2.782 ± 0.742	1.643 ± 0.625	1.348 ± 0.419
13	16	30	1.771 ± 0.413	1.361 ± 0.386	2.564 ± 1.167

in micron scale. Extending the ranges of the parameters was expected to help achieve the goal of nano-scale fiber production. Because of its dominant effect, the adjustment of molecular weight only, was expected to allow reduced fiber diameters. It was fixed, however, at its original lower limit for further investigation here, because fixing the molecular weight of PAN was expected to surface the effect of the other parameters, x_2, x_3 and x_4 and possibly to provide finer tuning for the resultant fiber diameter.

Among the remaining three variables, three different collector distances, x_4 were considered, at 8, 12 and 16 cm. At each collector distance, experiments in x_2 and x_3 domain (solution concentration and applied voltage, respectively) were carried out. Thirteen experiments of 2-D evaluations at each collector distance are shown schematically in Fig. 3. Nine of them marked by filled circles are the experimental settings defined by standard two-variable face-centered central composite design (FCCD). The other four marked by squares are to provide additional levels for the variables. The experimental
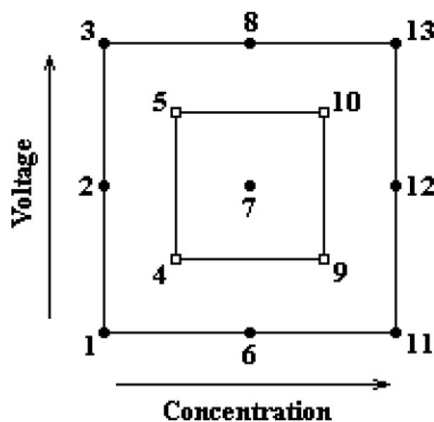
settings are summarized in Table 4. Note that the lower limits for the variables were lowered compared to the limits reported in Table 2.

Table 5
Parameter estimates and the statistical results of each cubic RS approximation for mean fiber diameter at three different collector distances[a]

Term	Estimate	p-Value	Summary of fit	
Collector distance: 8 cm				
Intercept, b_0	−32.69	0.011	Mean	1.059
x_2, b_1	9.94	0.007	RMSE	0.150
x_3, b_2	−0.74	0.086	R^2	0.990
x_2^2, b_3	−0.86	0.007		
$x_2 * x_3$, b_4	−0.01	0.834		
x_3^2, b_5	0.04	0.061		
x_2^3, b_6	0.02	0.007		
$x_2^2 * x_3$, b_7	0.003	0.028		
$x_2 * x_3^2$, b_8	−0.002	0.008		
x_3^3, b_9	−0.0003	0.0297		
Collector distance: 12 cm				
Intercept, b_0	19.53	0.107	Mean	0.820
x_2, b_1	−5.11	0.107	RMSE	0.222
x_3, b_2	−0.19	0.693	R^2	0.972
x_2^2, b_3	0.43	0.110		
$x_2 * x_3$, b_4	0.02	0.565		
x_3^2, b_5	0.01	0.843		
x_2^3, b_6	−0.01	0.121		
$x_2^2 * x_3$, b_7	−0.001	0.565		
$x_2 * x_3^2$, b_8	−0.0001	0.781		
x_3^3, b_9	−0.0001	0.864		
Collector distance: 16 cm				
Intercept, b_0	−1.55	0.862	Mean	0.874
x_2, b_1	0.20	0.931	RMSE	0.213
x_3, b_2	0.25	0.582	R^2	0.985
x_2^2, b_3	0.02	0.910		
$x_2 * x_3$, b_4	−0.07	0.118		
x_3^2, b_5	0.01	0.772		
x_2^3, b_6	0.0002	0.975		
$x_2^2 * x_3$, b_7	0.0003	0.840		
$x_2 * x_3^2$, b_8	0.002	0.038		
x_3^3, b_9	−0.0004	0.341		

[a] x_2: solution concentration, x_3: applied voltage.

Fig. 3. Design of experiments of two-variables, solution concentration x_2 and applied voltage x_3, at fixed collector distances x_4.
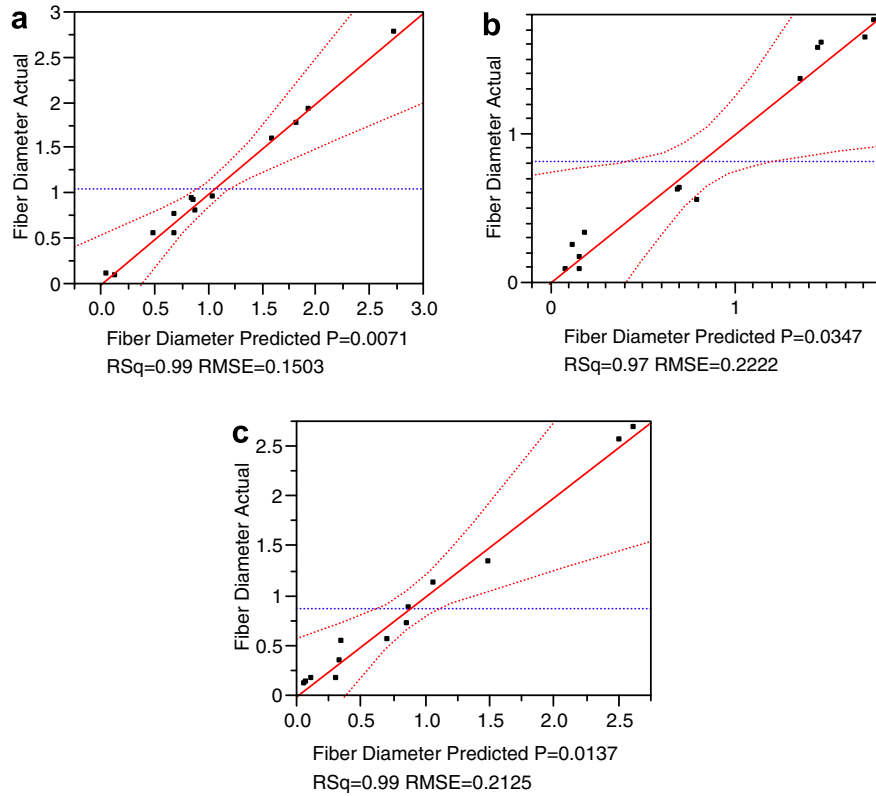
Fig. 4. Predicted versus actual mean fiber diameter plots (a) 8 cm colector distance, (b) 12 cm colector distance, and (c) 16 cm colector distance.

4.1. Results from response surface for mean fiber diameter

The data of 13 experiments represented in Fig. 3 were obtained by following the experimental procedure described in Section 2. At each collector distance, a total of 13 experiments, including five levels of both parameters, allow to fit a cubic RS model as a function of solution concentration and applied voltage, at fixed molecular weight,

$$\hat{y} = b_0 + b_1 x_2 + b_2 x_3 + b_3 x_2^2 + b_4 x_2 x_3 + b_5 x_3^2 + b_6 x_2^3$$
$$+ b_7 x_2^2 x_3 + b_8 x_2 x_3^2 + b_9 x_3^3 \qquad (2)$$

Response surfaces of the mean fiber diameter fitted to data of each collector distance are summarized in Table 5. The R^2 values, roughly around 0.98, illustrate that the models are able to explain 98% of the variability in the mean fiber diameter over the two-variable domain, at each collector distance. Furthermore, the p-values of concentration related terms in Eq. (2) suggest now the concentration, as well as the voltage, is a significant parameter as expected.

In addition to the statistical results, goodness of the cubic RS models can be graphically represented by the predicted versus the actual diameter plots, as illustrated in Fig. 4.

Relying on the goodness of the fit, mean fiber diameter was predicted on a 21×21 grid of the concentration versus voltage domain. For each collector distance associated cubic RS presented in Table 5 was utilized to prepare con-

tour plots of the predicted mean fiber diameter as illustrated in Fig. 5. Each contour visualizes the effects of concentration and voltage at the corresponding collector distance. In addition, comparison of the three contour plots shows the effect of the collector distance.

The contour plots indicate that the resultant fiber diameter is very responsive to the changes in concentration as expected and previously mentioned in several other studies [13,17,21,25,30,34,35]. It is also responsive to changes in voltage, but its effect depends on the level of solution concentration and collector distance. Similar outcomes consistent with our results were reported by Baumgarten [29] and Fennessey [36] for PAN; and Sukigara et al. [17] for Bombyx silk fibers. However, these contradict with the observations by Gu et al. [25]. In their experiments, diameter of the fibers did not change as they altered the voltage, at the collector distance where all of their experiments were carried out. This contradiction is attributed to the fact that the extent of the interaction of any two variables may depend on the third, as observed in this study. As we adjusted the collector distance, the contribution of voltage in fiber diameter formation was observed. For instance, at collector distance of 8 cm (Fig. 5a), fiber diameter is more sensitive to the changes in voltage up to 14% solution concentration, and its effect becomes negligible as level of concentration increases up to 16%. Moreover, at 12 cm and 16 cm collector distances (Fig. 5b and c), contour plots suggest that voltage has almost no and very little effect on fiber diameter formation, respectively. Therefore, voltage is
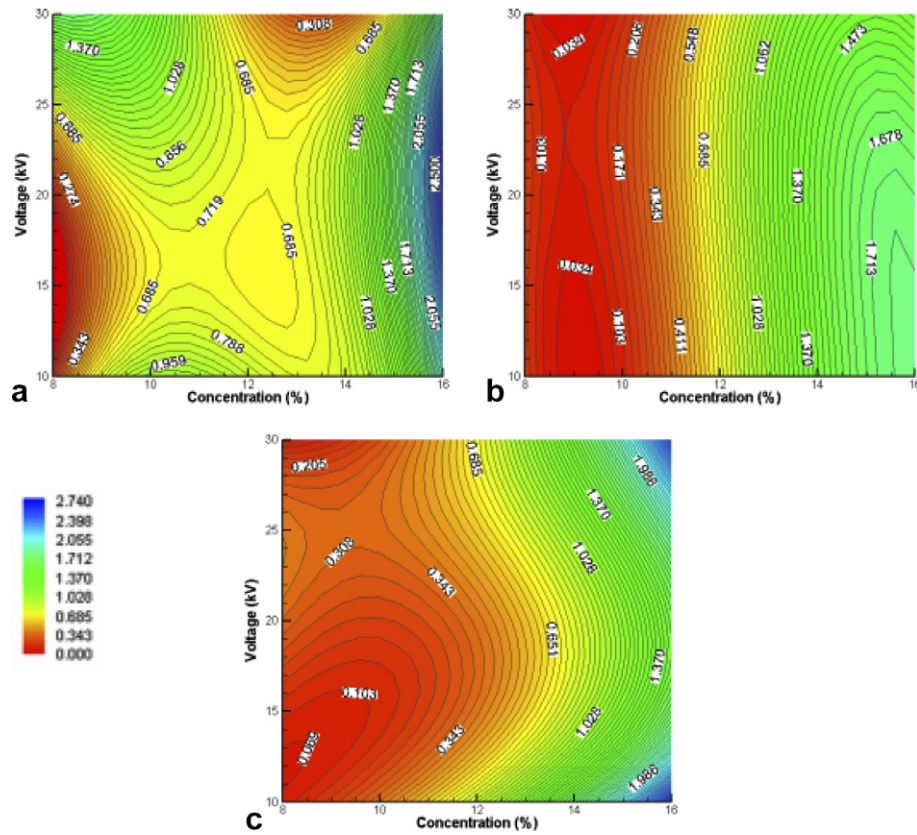
Fig. 5. Mean fiber diameter contour plots by predictions using RS approximations summarized in this figure (a) 8 cm collector distance, (b) 12 cm collector distance, and (c) 16 cm collector distance.

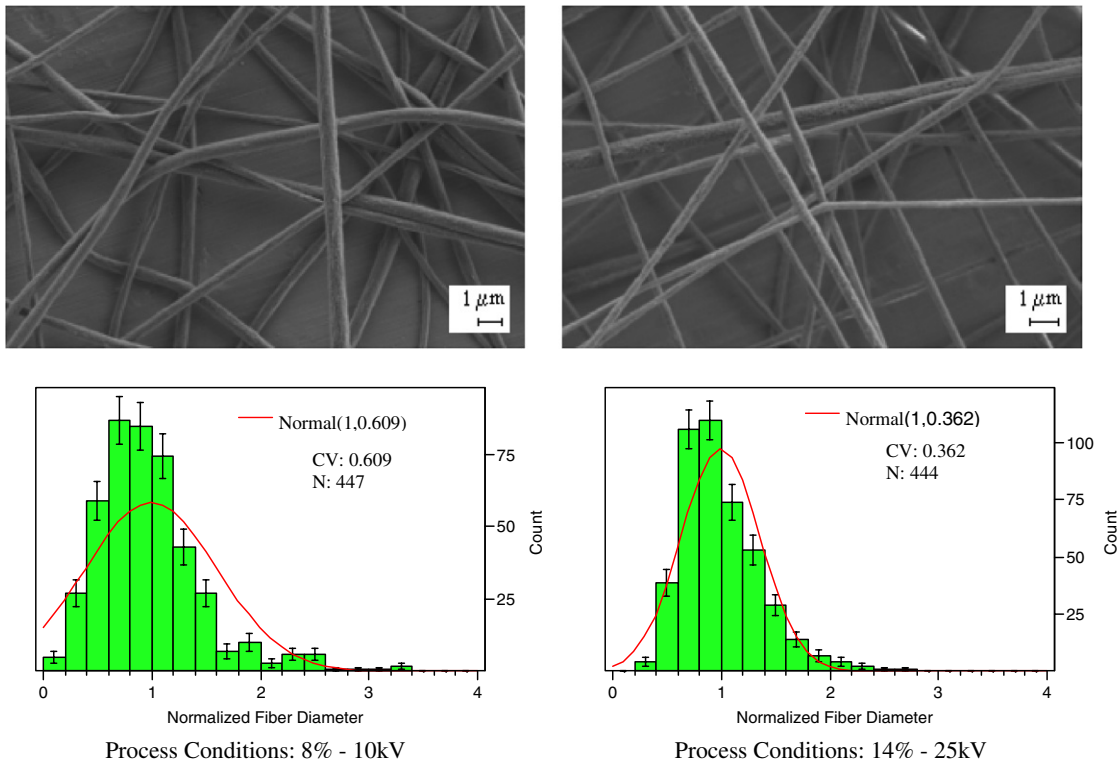Process Conditions: 8% - 10kV   Process Conditions: 14% - 25kV

Fig. 6. Scatter of diameter of fibers and its dependence on the process and material parameters (e.g. at collector distance 8 cm).
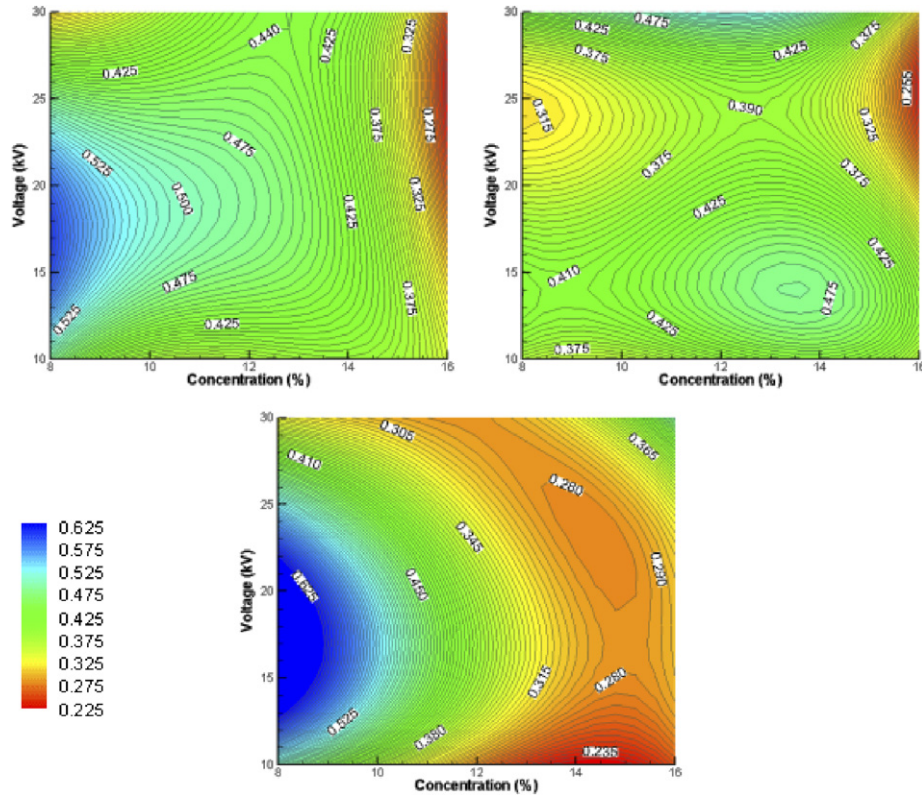
Fig. 7. Contour plots for coefficient of variation by predictions using cubic RS approximations, (a) 8 cm collector distance, (b) 12 cm collector distance, and (c) 16 cm collector distance.

a factor for fiber diameter, but at a different level of significance depending on the concentration and collector distance.

4.2. Results from response surface for coefficient of variation of fiber diameter

Recall that the measurement procedure uses SEM images over locations remote from each other on a non-woven mat of fibers. The image processing revealed that fibers produced at a given parameter settings exhibit scatter of the fiber diameter and the amount of scatter may also vary as a function of the parameters within the domain. For instance, at experimental condition of $x_2 = 8\%$, $x_3 = 10$ kV coefficient of variation (CV = standard deviation normalized with the experiment's mean fiber diameter) was CV = 0.609, while at experimental condition of $x_2 = 14\%$, $x_3 = 25$ kV, was CV = 0.362. The distributions of the fiber diameter normalized by the mean value at these settings are shown in Fig. 6. Based on the data collected at 13 experiments carried out on each collector distance, prediction of the scatter dependence on parameters was also investigated. Coefficient of variation at each experiment was first computed by normalizing the standard deviation with the experiment's mean fiber diameter. Then cubic RS model of Eq. (2) was fit to the coefficient of variation data of 13 experiments at each collector distance. The accuracy of

the RS approximations is reasonable with R^2 values of about 0.93. Contours of the coefficient of variation (CV) were also plotted as shown in Fig. 7. Contour plots of the mean fiber diameter and the CV together provide information on the correlation between the scatter and the fiber diameter. It appears that there is a negative correlation between the mean fiber diameter and the relative scatter (CV), that is the lower the mean fiber diameter, the higher is the scatter around it. This appears to be contradictory with the results by Gu et al. [25]. The major reason of this contradiction is attributed to the fact that the polymers synthesized differently, which yield polymers with different molecular weights. Difference in the molecular weight of these polymers exhibit a variation in the chain entanglement of the two polymers. Chain entanglements have a significant impact on the electrospinning process, deciding whether the jet breaks up into droplets, beads, or fibers, and they affect the geometry of these formations.

Coefficient of correlation based on the 21×21 grid predictions is about -0.89. As for the CV dependence on the parameters, the plots suggest that scattering increases at low concentrations and it becomes less as the concentration increases. In addition to this, scattering is affected by both concentration and voltage at lower edges and voltage has less effect in high concentration edge. Furthermore, three contour plots conjointly suggest that scattering is also affected by variations in the collector distance.

4.3. Parameter space narrowed down by RS for nano-scale PAN fiber production

At 8 cm collector distance, the mean fiber diameter predictions on the solution concentration of 8% at low voltage values are negative. This is attributed to RMSE being about 0.150, which is substantially high compared to low fiber diameter regions. The RMSE is, in fact, quite reasonable considering the fact that least squares procedure provides a global approximation over a range from nano-scale to micro-scale, and it is about 15% of the mean of the whole domain. This is an indication that the cubic RS constructed in this domain is not sufficient to make precise predictions for the nano-scale fibers. It is quite useful, however to determine potential regions/windows of parameter domain in production of nano-scale fibers. Such a windowing may be further investigated for finer predictions of nano-scale ranges. Overall, it was observed that mean fiber diameter decreases with concentration. As the concentration is decreased as does the viscosity. As the number of solvent molecules increase, the lesser amount of polymer chains make the surface tension dominate the electrospun jet that results in thinner fibers or bead formation along the fibers [33]. Yet, as the concentration increases charges on the electrospinning jet will be able to stretch the polymer solution; thus, the polymer chain; hence, thicker fibers are formed. The contour plots further suggest the possible concentration and voltage ranges as 8–10% and 10–20 kV, respectively, for nano-scale fiber production. It is also observed that as collector distance is increased, nano-scale fiber formation range also increases.

5. Concluding remarks

An experimental investigation of electrospinning process and material parameters to produce PAN fibers was carried out. The goal was to investigate the interactive effects of the parameters on the resultant fiber and to establish a prediction scheme for the domain/window of the parameters where targeted PAN fiber diameter can be achieved. The planning of the experiments, the analyses of the results and the predictions were performed within the context of Response Surface Methodology featuring design of experiments and linear regression analysis.

Sets of experiments were performed at three collector distances each allowing evaluation of solution concentration and applied voltage two-variable domain associated with the collector distances. Contour plots of mean and coefficient of variation of the formed fiber diameter, on the solution concentration and applied voltage parameter domain, were created by the cubic polynomial response surface models. The predictions of the empirical models and contour plots suggest the following conclusions in electrospinning of polyacrylonitrile/DMF system studied here:

– Applied voltage was found to be an insignificant factor when the concentration level was high. That is, control of fiber diameter in micrometer scale may be provided by concentration alone. However, voltage was found to be an eminent parameter, depending on the concentration and collector distance levels, and this observation demonstrates the interactive effects of the parameters.
– Collector distance, as well as both voltage and concentration were found to be significant in nano-scale fiber production. The collector distance may be increased in favor of reducing the fiber diameter.
– The fiber diameter and the coefficient of variation are negatively correlated. Scatter of the diameter of nano-scale fiber mats is predicted to be high.
– The domain of potential nano-scale fiber was predicted to be in low concentration and voltage ranges (8–10% and 10–20 kV, respectively, for PAN/DMF with molecular weight of about 75,000 g/mol due to Mark-Houwink equation).

Appendix. Response surface methodology

Response surface methodology [37,27] assumes that the RS expression is exact and that the differences (called residuals) between the data and the RS are due to uncorrelated, normally distributed random noise of magnitude $\in$ in the experiments. Based on this assumption, if the true response is given in terms of n_b coefficients, β_is and assumed shape functions f_i (usually monomials) as

$$y(\mathbf{x}) = \sum_{i=1}^{n_b} \beta_i f_i(\mathbf{x}) + \in \tag{3}$$

then the RS approximation $\hat{y}$ is written as

$$\hat{y}(\mathbf{x}) = \sum_{i=1}^{n_b} b_i f_i(\mathbf{x}) \tag{4}$$

where b_is are unbiased estimates of the β_is.

The difference (residual) e_j between the data y_j for the jth point $\mathbf{x}_j$ and the estimate defined in (4) is given in matrix form for n_d data points as

$$\mathbf{e} = \mathbf{y} - \mathbf{Xb} \tag{5}$$

where $\mathbf{X}$ is the matrix whose component (j, i) is $f_i(\mathbf{x}_j)$. The coefficient vector $\mathbf{b}$ in (5) is solved for the minimum residual vector in a least-square sense, to obtain

$$\mathbf{b} = (\mathbf{X}^T \mathbf{X})^{-1} \mathbf{X}^T \mathbf{y} \tag{6}$$

where superscript T denotes the transpose operation. An unbiased estimate of the noise s (the root mean square error estimator, RMSE) in the data is given as

$$s = \sqrt{\frac{\mathbf{y}^T \mathbf{y} - \mathbf{b}^T \mathbf{X}^T \mathbf{y}}{n_d - n_b}} \tag{7}$$

In addition to s, the quality of the approximation is often measured by the coefficient of multiple determination, R^2. An R^2 value larger than 0.9 is typically required for an adequate approximation. R^2 is a measure of the proportion of total variation of the values of y_i about the mean value of the response $\bar{y}$ explained by the fitted model [37]. This coefficient is given as

$$R^2 = \frac{\sum_{j=1}^{n_d}(\hat{y}_j - \bar{y})^2}{\sum_{j=1}^{n_d}(y_j - \bar{y})^2} \tag{8}$$

The variance–covariance matrix of the vector of estimates **b** is estimated as

$$\mathrm{Var}(\mathbf{b}) = (\mathbf{X}^{\mathrm{T}}\mathbf{X})^{-1}s^2 \tag{9}$$

The estimated standard deviation of ith coefficient b_i (called standard error) is denoted by s_i, and is obtained as the positive square root of the ith term of the diagonal of $\mathrm{Var}(\mathbf{b})$. The hypothesis about the individual coefficients in the model can be tested by comparing the coefficient estimates to their respective estimated standard errors. Student's t-statistic

$$t = \frac{b_i}{s_i} \tag{10}$$

is used to test the null hypothesis H_0: $\beta_i = 0$. This is a two-tailed test against the alternatives in each direction.

The *p-value* is the smallest significance level for which any of the tests would have rejected the null hypothesis [38]. It represents an index of the reliability of a result. In case of a null hypothesis H_0: $\beta_i = 0$ it is likely that the coefficient of a particular term is actually zero rather than the value calculated. The smaller *p-value* gets, the smaller is the chance of being wrong in accepting that the coefficient is different than zero, and that there is a relation between the response and the associated regression terms. The *p-value* for H_0: $\beta_i = 0$ can be determined by comparing the t-statistic obtained by (10) with the values in statistical tables of the Student distribution [27]. Probabilities of less than 0.05 are considered as significant evidence that the coefficient is not zero.

References

[1] Li W-J, Laurencin CT, Caterson EJ, Tuan RS, Ko FK. Electrospun nanofibrous structure: a novel scaffold for tissue engineering. J Biomed Mater Res 2001;60:613–21.

[2] Bölgen N, Menceloglu YZ, Acatay K, Vargel I. Pis Journal of Biomaterials Science PE, E. In vitro and in vivo degradation of non-woven materials made of poly(ε-caprolactone) nanofibers prepared by electrospinning under different conditions. J Biomater Sci Polym Ed 2005;16:1537–55.

[3] Gibson PW, Schreuder-Gibson HL, Rivin D. Electrospun fiber mats: transport properties. AIChE J 1999;45:190–5.

[4] Kameoka J, Verbridge SS, Liu H, Czaplewski DA, Craighead HG. Fabrication of suspended silica glass nanofibers from polymeric materials using a scanned electrospinning source. NanoLetters 2004;4:2105–8.

[5] Pawlowski KJ, Belvin HL, Raney DL, Su J, Harrison JS, Siochi EJ. Electrospinning of a micro-air vehicle wing skin. Polymer 2003;44: 1309–14.

[6] Acatay K, Simsek E, Ow-Yang C, Menceloglu YZ. Tunable, Superhydrophobically Stable Polymeric Surfaces by Electrospinning. Angew Chem Int Ed 2004;43:5210–3.

[7] Formhals A. US Patent. 1975504; 1934.

[8] Doshi J, Reneker DH. Electrospinning process and applications of electrospun fibers. J Electrostat 1995;35:151–60.

[9] Reneker DH, Chun I. Nanometre diameter fibres of polymer, produced by electrospinning. Nanotechnology 1996;7:216–23.

[10] Deitzel JM, Kleinmeyer J, Harris D, Tan NCB. The effect of processing variables on the morphology of electrospun nanofibers and textiles. Polymer 2001;42:261–72.

[11] Reneker DH, Fong H, AL Y, Koombhongse S. Bending instability of electrically charged liquid jets of polymer solutions in electrospinning. J Appl Phys 2000;87:4531.

[12] Li D, Xia Y. Electrospinning of nanofibers: reinventing the wheel? Adv Mater 2004;16:1151.

[13] Kattamuri N, Sung C. Uniform polycarbonate nanofibres produced by electrospinning. Macromolecules 2004;3:425.

[14] Fridrikh SV, Yu JH, Brenner MP, Rutledge GC. Controlling the fiber diameter during electrospinning. Phys Rev Lett 2003;90: 1445502–04.

[15] Larrondo L, Manley J. Electrostatic fiber spinning from polymer melts. I. Experimental observations on fiber formation and properties. J Polym Sci, Part B: Polym Phys 1981;19: 909.

[16] Rutledge GC, Li Y, Fridrikh S, Warner SB, Kalayci VE, Patra P. Electrostatic spinning and properties of ultrafine fibers; 2001.

[17] Sukigara S, Gandhi M, Ayutsede J, Micklus M, Ko F. Regeneration of Bombyx Mori silk by electrospinning. Part 2. Process optimization and empirical modelling using response surface methodology. Polymer 2004;45:3701–8.

[18] Demir MM, Yilgor I, Yilgor E, Erman B. Electrospinning of Polyurethane fibers. Polymer 2002;43:3303–9.

[19] Dzenis Y. Spinning continuous fibers for nanotechnology. Science 2004;304:1917.

[20] Kwon IK, Kidoaki S, Matsuda T. Electrospun nano- to microfiber fabrics made of biodegradable copolyesters: structural characteristics, mechanical properties and cell adhesion potential. Biomaterials 2004;26:3929–39.

[21] El-Aufy AK. Nanofibers and nanocomposites of poly(3,4-ethylene dioxythiophene)/poly(styrene sulfonate) by electrospinning; 2004.

[22] Simsek E, Acatay K, Menceloglu YZ. Effect of perfluoroacrylate ratio on the generation of stable superhydrophobic surfaces displaying low contact angle hysteresis, vol. 229. American Chemical Society; 2005.

[23] Reneker DH, Shin C, Chase GG. Recycled expanded polystyrene nanofibers applied in filter media. Colloid Surf A: Physicochem Eng Aspects 2005;262:211–5.

[24] Grafe TH, Graham KM. Nanofiber webs from electrospinning. Nonwovens in filtration – fifth international conference; 2003.

[25] Gu SY, Ren J, Vansco GJ. Process optimization and empirical modeling for electrospun polyecrylonitrile (PAN) nanofiber precursor of carbon nanofibers. Eur Polym J 2005.

[26] Papila M, Haftka RT. Response surface approximations: noise, error repair, and modelling errors. AIAA J 2000;38:2336–43.

[27] Khuri AI, Cornell JA. Response surfaces: designs and analyses. New York: Marcel Dekker Inc.; 1996.

[28] Montgomery Ma. Response surface methodology. Wiley; 1997.

[29] Baumgarten PK. Electrostatic spinning of acrylic fibers. J Colloid Interface Sci 1971;36:71.

[30] Mo XM, Xu CY, Kotaki M, Ramakrishna S. Electrospun P(LLA-CL) nanofiber: a biomimetic extracellular matrix for smooth muscle cell and endothelial cell proliferation. Biomaterials 2004;25:1883–90.

[31] Katti DS, Robinson KW, Ko FK, Laurencin CT. Bioresorbable nanofiber-based systems for wound healing and drug delivery: optimization of fabrication parameters. J Biomed Mater Res Part B: Appl Biomater 2004;70B:286–96.

[32] Brandrup J, Immergut EH, Grulke EA. Polymer handbook. Canada: Wiley; 1999.

[33] Ramakrishna S, Kujihara K, Teo W-E, Lim T-C, Ma Z. An introduction to electrospinning and nanofibers. Hackensack: World Scientific Co. Pvt. Ltd.; 2005.

[34] Matthews JA, Wnek GE, Simpson DG, Bowlin GL. Electrospinning of collagen nanofibers. Biomacromolecules 2003;3:232–8.

[35] Ryu YJ, Kim HY, Lee KH, Park HC, Lee DR. Transport properties of electrospun nylon 6 nonwoven mats. Eur Polym J 2003;39:1883–9.

[36] Fennessey SF, Farris RJ. Fabrication of aligned and molecularly oriented electrospun polyacrylonitrile nanofibers and the mechanical behavior of their twisted yarns. Polymer 2004;45:4217.

[37] Myers RH, Montgomery DC. Response surface methodology: process and product optimization using designed experiments. New York: John Wiley and Sons; 1995.

[38] Stark PB. SticiGui: Statistics Tools for Internet and Classroom Instruction with a Graphical User Interface. Available from: <http://oz.berkeley.edu/users/stark/SticiGui>. Accessed 31 January 2007.